



Oxygenated xanthenes as P-glycoprotein modulators at the intestinal barrier: in vitro and docking studies

Vera Silva¹ · Eva Gil-Martins¹ · Carolina Rocha-Pereira¹ · Agostinho Lemos² · Andreia Palmeira² · Ploenthip Puthongking³ · Emília Sousa² · Maria de Lourdes Bastos¹ · Fernando Remião¹ · Renata Silva¹

Received: 13 December 2019 / Accepted: 4 April 2020 / Published online: 29 April 2020
© Springer Science+Business Media, LLC, part of Springer Nature 2020

Abstract

P-glycoprotein (P-gp) induction and/or activation have been proposed as therapeutic strategies in intoxication scenarios, by reducing the intestinal absorption of xenobiotics, including drugs. Oxygenated xanthenes (OXs) have been described as P-gp modulators and, therefore, the main goals of this study were to: (a) investigate the potential modulatory effect of six OXs on P-gp expression and activity in SW480 cells; (b) validate these cells for the screening/identification of P-gp inducers/activators; (c) explore the potential OXs-mediated protective effects against the cytotoxicity of mitoxantrone (MTX), a toxic P-gp substrate. Four OXs (**OX2**, **OX4**, **OX5**, and **OX6**) increased P-gp expression 24 h after exposure. However, a lack of correlation between P-gp expression and activity was observed for **OX1** and **OX4**. In addition, after a short incubation with the P-gp fluorescent substrate, rhodamine 123, all the studied OXs, except **OX3**, efficiently and immediately increased P-gp activity, suggesting their potential as P-gp activators. Despite these results, OXs failed to afford protection against MTX-induced cytotoxicity. Docking simulations performed in a human P-gp model revealed that the lack of protection may be explained by the different binding locations of OXs and MTX within the P-gp drug-binding pocket. In conclusion, the in vitro results confirmed OXs potential for P-gp induction and/or activation and suggested SW480 cells as a suitable in vitro model for these studies. However, P-gp activation did not protect SW480 cells against MTX cytotoxicity. *In silico* studies suggested the different binding locations as a limiting step in the P-gp-mediated efflux of its substrates under P-gp activation.

Supplementary information The online version of this article (<https://doi.org/10.1007/s00044-020-02544-1>) contains supplementary material, which is available to authorized users.

✉ Vera Silva
veralssilva17@gmail.com

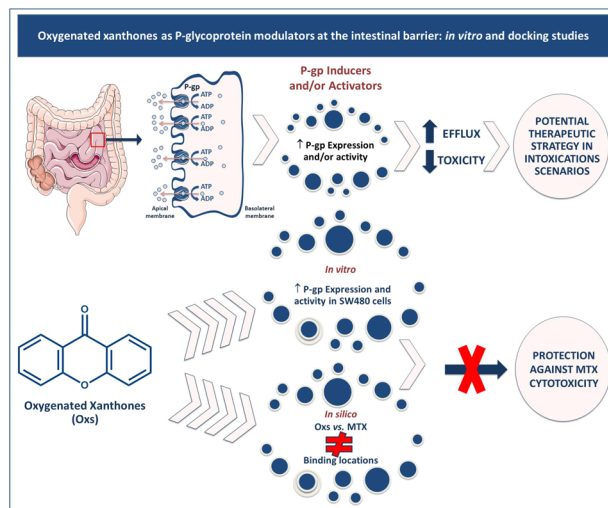
✉ Renata Silva
rsilva@ff.up.pt

¹ UCIBIO/REQUIMTE, Laboratório de Toxicologia, Departamento de Ciências Biológicas, Faculdade de Farmácia, Universidade do Porto, Rua Jorge Viterbo Ferreira, 228, 4050-313 Porto, Portugal

² CIIMAR, Laboratório de Química Orgânica e Farmacêutica, Departamento de Ciências Químicas, Faculdade de Farmácia, Universidade do Porto, Rua Jorge Viterbo Ferreira, 228, 4050-313 Porto, Portugal

³ Faculty of Pharmaceutical Sciences, Khon Kaen University, Khon Kaen 40002, Thailand

Graphical Abstract



Keywords P-glycoprotein · Induction · Activation · Oxygenated xanthenes · Intestinal barrier

Introduction

ATP-binding cassette (ABC) transporters are a superfamily of carrier proteins that play a crucial role in cell physiology and homeostasis, promoting the efflux of substrates by using the energy resultant from ATP hydrolysis (Sharom 2011; Silva et al. 2015a; b; Gameiro et al. 2017). P-glycoprotein (P-gp) is the best characterized member of the ABC superfamily, having an ubiquitous distribution in the human body, with greater relevance in barrier and excretory tissues (Sharom 2011; Silva et al. 2015a; b; Gameiro et al. 2017). P-gp location allows a better understanding of its role in the pharmaco(toxico)kinetic processes, such as absorption, distribution, metabolism, elimination, and transport (ADMET). Undeniably, P-gp acts as a physiological barrier by conferring cellular protection through the efflux of endogenous and exogenous compounds (Sharom 2011; Silva et al. 2015a; b; Gameiro et al. 2017), a phenomenon that explains its important role in altering the bioavailability of xenobiotics recognized as its substrates, resulting in an extensive reduction of their action and/or toxicity (Fromm 2004; Sharom 2011; Mizutani et al. 2012; Silva et al. 2015a; b).

The intestinal absorption of compounds occurs mainly at the small intestine, especially in the polarized enterocytes of the duodenum and jejunum, due to its large surface area (Pang 2003; Oostendorp et al. 2009). However, the intestine role in the absorption process is also explained by the presence of efflux and influx transporters, located at the apical and basolateral membranes of the intestinal cells (Pang 2003, Varma et al. 2010). P-gp is highly expressed at the apical membrane of enterocytes and, by promoting the

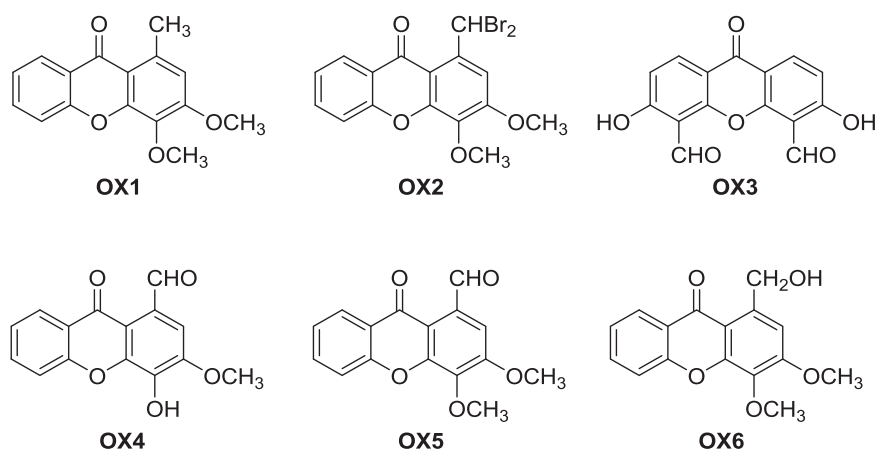
cellular extrusion of toxic substances against their concentration gradient, transporting them towards the lumen of the gastrointestinal tract, this protein confers protection against toxic molecules by avoiding their systemic absorption (Silva et al. 2015a; b).

According to the previously mentioned P-gp physiological role, several studies have been conducted in recent years with the purpose of discovering new chemical entities able to modulate P-gp, either through its induction and/or activation. In fact, rifampicin derivatives (Vilas-Boas et al. 2013a; b), but particularly several xanthonic and thioxanthonic derivatives were synthesized and tested in vitro (Silva et al. 2014a; b, 2015a; b; Lopes et al. 2018; Martins et al. 2019) and in vivo (Rocha-Pereira et al. 2019), as potential P-gp inducers/activators to be used as antidotes in intoxication scenarios, by reducing the absorption and increasing the elimination of toxic P-gp substrates.

Xanthenes are oxygenated heterocyclic compounds belonging to the dibenzo- γ -pyrone class and can be found as secondary metabolites in plants, fungi, lichens, and bacteria (Masters and Brase 2012). Furthermore, it is possible to create an enormous number of synthetic derivatives from a xanthonic scaffold, by adding different side chains to the backbone (Pinto et al. 2005), which can be investigated for their ability to modulate P-gp expression and/or activity.

Therefore, considering the vital P-gp physiological role in the elimination of harmful compounds, the main goal of the present work was to evaluate the effect of six oxygenated xanthenes (OX 1–6, Fig. 1) on P-gp expression and activity, using SW480 cells as an in vitro model. Moreover, we also aimed to assess whether these xanthenes, by

Fig. 1 Chemical structures of the oxygenated xanthenes **OX 1–6** investigated in this study



modulating P-gp expression and/or activity, were able to afford protection against the cytotoxicity induced by mitoxantrone (MTX), a potent and extremely toxic P-gp substrate. These OXs were previously screened for their P-gp modulatory effect in the Caco-2 cells model, demonstrating their potential for P-gp modulation (Martins et al. 2019). However, the modulation of P-gp expression levels appears to be cell and tissue specific. Therefore, with these studies, we also sought to validate SW480 cells, human colon cancer cells, as a suitable *in vitro* model to be used in the screening and identification of P-gp inducers and/or activators.

Experimental design, materials, and methods

Materials

Reagents used in cell culture, including Dulbecco's modified Eagle's medium (DMEM) without glucose, DMEM with 4.5 g/L glucose, L-glutamine, rhodamine 123 (RHO 123), zosuquidar (ZOS), 3-(4,5-dimethylthiazol-2-yl)-2,5-diphenyl tetrazolium bromide (MTT), neutral red (NR) solution, MTX, and dimethyl sulfoxide (DMSO) were obtained from Sigma-Aldrich (St. Louis, MO, USA). Sodium bicarbonate and glucose were purchased from Merck (Darmstadt, Germany). Triton™ X-100 detergent solution was acquired from Thermo Fisher Scientific (Waltham, MA, USA). Fetal bovine serum (FBS), non-essential amino acids (NEAA), antibiotic (10,000 U/mL penicillin, 10,000 µg/mL streptomycin), hank's balanced salt solution with or without calcium and magnesium [HBSS (+/+) or HBSS (-/-), respectively], phosphate-buffered saline solution (PBS) and 0.25% trypsin/1 mM ethylenediamine tetraacetic acid (EDTA) were purchased from Gibco Laboratories (Lenexa, KS, USA). P-gp monoclonal antibody (clone UIC2) conjugated with

phycoerythrin (PE), was purchased from Abcam (Cambridge, United Kingdom). Reagents used in flow cytometry, namely, the cleaning solution, decontamination solution, and flow cell extended clean solution were purchased from BD Biosciences (San Jose, CA, USA). All the reagents used were of analytical grade or of the highest grade available.

Oxygenated xanthenes **OX 1–6** (Fig. 1) were synthesized and characterized according to previous procedures (Fernandes et al. 1998; Cruz et al. 2017; Resende et al. 2018; Gomes et al. 2019; Lemos et al. 2019; Martins et al. 2019). A 50.0 mM stock solution of each OX was prepared in DMSO. All stock solutions were stored at -20°C and freshly diluted on the day of the experiment in fresh cell culture medium (ensuring that DMSO did not exceed 0.1% DMSO concentration of the exposure media).

SW480 cell culture

SW480 cells were obtained from the American Type Culture Collection (ATCC; Manassas, VA, USA), and were routinely cultured in 75 cm² flasks using DMEM supplemented with 0.9 g/L glucose, 3.7 g/L NaHCO₃, 10% FBS, 1% L-glutamine, and 1% antibiotic (10,000 U/mL penicillin, 10,000 µg/mL streptomycin). Cells were routinely maintained in a 5% CO₂–95% air atmosphere at 37 °C and, to maintain an adequate cell growth, the medium was changed every 2–3 days. Cultures were passed weekly by trypsinization (0.25% trypsin/1 mM EDTA). In all experiments, cells were seeded at a density of 50,000 cells/cm² and used 3 days after seeding, when confluence was reached. The cells used in all experiments were taken between the 12th and 22nd passages.

Caco-2 cell culture

Caco-2 cells were obtained from the European Collection of Authenticated Cell Culture (ECACC, UK) and routinely cultured in 75 cm² flasks using DMEM with 4.5 g/L glucose

supplemented with 10% heat-inactivated FBS, 100 μM NEAA, and 1% antibiotic (10,000 U/mL penicillin, 10,000 $\mu\text{g}/\text{mL}$ streptomycin). Cells were maintained in a 5% CO_2 –95% air atmosphere at 37 °C and the medium was changed every 2–3 days. Cultures were passaged weekly by trypsinization (0.25% trypsin/1 mM EDTA). In all experiments, the cells were seeded at a density of 60,000 cells/ cm^2 and used 3 days after seeding, when confluence was reached. The cells used in all experiments were taken between the 54th and 64th passages.

Oxygenated xanthenes cytotoxicity

Oxygenated xanthenes (0–50 μM) cytotoxicity was evaluated, in SW480 cells, by MTT reduction and NR uptake assays, 24 h after exposure. For that purpose, SW480 cells were seeded at a density of 50,000 cells/ cm^2 into 96-well plates and exposed, after reaching confluence, to the tested OXs [OX 1–6 (0–50 μM)], in fresh cell culture medium. Triton™ X-100 (0.1%) was used as positive control.

MTT reduction assay

The MTT reduction assay is a colorimetric assay used to measure mitochondrial dysfunction, which is based on the reduction of the water-soluble yellow tetrazolium dye, MTT, to a water-insoluble blue to purple formazan product, by mitochondrial succinic dehydrogenases (Barbosa et al. 2014). Mitochondrial dehydrogenases of viable cells cleave the tetrazolium ring, reducing the tetrazolium dye into blue/purple and water-insoluble formazan crystals, which can be solubilized in an organic solvent and measured at 550 nm. Thus, it is predictable that formazan formation is directly proportional to the number of metabolically viable cells in culture (Borenfreund et al. 1988).

After the exposure period (24 h), the cell culture medium was removed, followed by the addition of fresh cell culture medium containing 0.3 mg/mL MTT, and incubation at 37 °C, in a humidified 5% CO_2 –95% air atmosphere, for 45 min. After this incubation period, the cell culture medium was removed, and the formed formazan crystals dissolved in 100% DMSO. The absorbance was measured at 550 nm in a multiwell plate reader (PowerWaveX BioTek Instruments, Vermont, USA). The percentage of MTT reduction relatively to that of the control cells (0 μM) was used as the cytotoxicity measure. Six independent experiments were performed, in triplicate.

Neutral Red uptake assay

The NR assay is based on the ability of viable cells to incorporate and bind the supravital dye NR into the lysosomes and, thus, the amount of NR dye incorporated into the

cells represents their lysosomal functionality, providing a quantitative estimation of the number of viable cells in a culture (Arbo et al. 2014; Silva et al. 2015a; b). The dye is then extracted from the viable cells using an acidified ethanol solution, and the absorbance of the solubilized dye is quantified using a spectrophotometer (Repetto et al. 2008).

After the exposure period (24 h), the cell culture medium was removed, followed by the addition of fresh cell culture medium containing 50 $\mu\text{g}/\text{mL}$ NR, and incubation at 37 °C, in a humidified 5% CO_2 –95% air atmosphere, for 1 h.

After this incubation period, the cell culture medium was removed, the dye absorbed only by viable cells extracted with absolute ethyl alcohol/distilled water (1:1) with 5% acetic acid, and the absorbance measured at 540 nm in a multiwell plate reader (PowerWaveX BioTek Instruments, Vermont, USA). The percentage of NR uptake relatively to that of the control cells (0 μM) was used as the cytotoxicity measure. Six independent experiments were performed, in triplicate.

Flow cytometry analysis of P-glycoprotein expression

P-gp expression was evaluated by flow cytometry, using a P-gp monoclonal antibody (UIC2 clone conjugated with PE), as previously described (Vilas-Boas et al. 2011; Silva et al. 2014a; b; Lopes et al. 2018; Martins et al. 2019). For that purpose, SW480 cells were seeded onto 48 well plates, at a density of 50,000 cells/ cm^2 and exposed, 3 days after seeding, to a noncytotoxic concentration (20 μM) of the tested OX 1–6, in fresh cell culture medium, for 24 h. Twenty-four hours after exposure, the cells were washed with HBSS (–/–) and harvested by trypsinization (0.25% trypsin/1 mM EDTA) to obtain a cell suspension. The cell suspension was then transferred to eppendorf tubes, centrifuged (130 g for 7 min, at 4 °C) and resuspended in HBSS (+/+) buffer containing the P-gp antibody. The antibody dilution used in this experiment was applied according to the manufacturer's instructions for flow cytometry. The cells were then incubated for 1 h, at 37 °C, in the dark, and under gentle shaking. After this incubation period, the cells were washed twice with HBSS (+/+), with intercalated centrifugations (130 g, for 7 min, at 4 °C) and kept on ice until analysis. Cells were then resuspended on ice-cold PBS (–/–) buffer immediately before the cytometer analysis. Fluorescence measurements of isolated cells were taken with a BD Accuri™ C6 flow cytometer (BD Biosciences, CA, USA), equipped with the FCS Express analysis software. The fluorescence of the UIC2-PE antibody was measured by a 585 \pm 40 nm band-pass filter (FL2). Logarithmic fluorescence was recorded and displayed as a single parameter histogram and based on the acquisition of data for at least 20,000 cells. The parameter used for comparison

was the mean fluorescence intensity (MFI), calculated as percentage of control cells (0 μM). The cells autofluorescence (unlabeled cells with or without the tested OXs) was also evaluated in every experiment in order to eliminate its potential contribution to the analyzed fluorescence signals. Six independent experiments were performed, in duplicate. Mouse IgG2a-PE was used as an isotype-matched negative control to estimate nonspecific binding of the PE-labeled anti-P-gp antibody (UIC2-PE).

Evaluation of P-glycoprotein transport activity

The OXs 1–6 effects on P-gp transport activity were evaluated using the well-known P-gp fluorescent substrate, RHO 123, and a specific third-generation P-gp inhibitor, ZOS. RHO 123 accumulation/efflux assays are common experiments used to directly evaluate P-gp activity by measuring RHO 123 intracellular fluorescence (Vilas-Boas et al. 2011, 2013a; b; Silva et al. 2014a; b, 2015a; b; Lopes et al. 2018). For that purpose, two different protocols were used: (a) RHO 123 accumulation in cells preexposed to OXs for 24 h; (b) RHO 123 accumulation in the presence of the tested OXs for 90 min.

In protocol A, RHO 123 accumulation was evaluated in cells preexposed to the tested OXs for 24 h. In this protocol, the cell culture medium containing the OXs was removed (24 h after exposure), the cells washed with HBSS (+/+) and, subsequently, submitted to a RHO 123 accumulation protocol in the absence of the tested compounds. Therefore, the measured RHO 123 intracellular fluorescence allows to assess whether potential increases (or decreases) in P-gp protein expression levels induced by the tested OXs, after a pre-exposure of 24 h, can be translated into the corresponding increases (or decreases) in pump activity, given the long period of preincubation with the tested compounds (24 h).

In protocol B, the tested OXs were added (except in the controls) 30 min prior to addition of the fluorescent substrate, RHO 123, and remained in contact with the cells during all the substrate accumulation period. This protocol aims to detect immediate effects of the tested compounds on P-gp activity as a result of a direct activation or inhibition of the pump. Therefore, in this case, the measured RHO 123 intracellular fluorescence reflects a direct P-gp activation (or inhibition), without the possible contribution of an increased (or decreased) expression of the pump, given the short contact period between the tested compounds and the cells (total time of contact of 2 h, which corresponds to the 30 min of preincubation plus 90 min of simultaneous incubation with the P-gp substrate) (Silva et al. 2014a; b, 2015a; b). In both protocols, P-gp activity was assessed in the presence and absence of ZOS (5 μM), a third-generation P-gp inhibitor. Correspondingly, and in both cases, P-gp activity was evaluated through the ratio between the

fluorescence intensity (FI) after inhibited RHO 123 accumulation (IA-inhibited accumulation in the presence of ZOS) and the FI of normal non-inhibited RHO 123 accumulation (NA, in the absence of the P-gp inhibitor) (Eq. (1)), and the results were expressed as percentage of control cells (0 μM). When P-gp activity increases, the amount of RHO 123 that is pumped out of the cells is higher and, consequently, accompanied by a decrease in the FI due to the corresponding decrease in the intracellular RHO 123 content (Silva et al. 2015a; b). Therefore, a higher RHO 123 accumulation ratio (Eq. (1)) is a consequence of a smaller FI under NA conditions, which results from a higher P-gp activity since the dye is being pumped out of the cells during the accumulation phase. In contrast, when P-gp activity decreases, the ratio FI_{IA}/FI_{NA} will be lower, since a higher FI under normal conditions (FI_{AN}) will be detected, because of the decreased RHO 123 efflux.

$$\text{Rho123 Accumulation} = \frac{FI \text{ of RHO123 accumulation under P-gp inhibition (IA)}}{FI \text{ of RHO123 accumulation under normal conditions (NA)}} \quad (1)$$

Eq. (1): P-gp activity assessed by the ratio between the amount of RHO 123 accumulated in the presence of the inhibitor (10 μM ZOS) and the amount of RHO 123 accumulated in the absence of P-gp inhibition. Fluorescence intensity (FI).

Zosuquidar and RHO 123 cytotoxicity

Prior to the evaluation of the effects of the OXs (OX 1–6) under study on P-gp activity, the cytotoxicity of both the P-gp fluorescent substrate (RHO 123) and the P-gp inhibitor (ZOS) was assessed. For that purpose, the SW480 cells were seeded at a density of 50,000 cells/cm² into 96-well plates and exposed, after reaching confluence, to ZOS (0–10 μM) and RHO 123 (0–5 μM) in fresh cell culture medium. Subsequently, the plates exposed to ZOS were incubated, at 37 °C, in a humidified 5% CO₂–95% O₂ air atmosphere for 24 h, while for the plates exposed to RHO 123, the cytotoxicity was evaluated 2 h after exposure. Following the respective incubation periods, the cytotoxicity of both ZOS and RHO 123 was evaluated by using the MTT reduction and NR uptake assays, as described in the sections “MTT reduction assay” and “Neutral Red uptake assay”, respectively. Four to six independent experiments were performed, in triplicate.

RHO 123 accumulation assay in cells preexposed to xanthenes for 24 h (Protocol A)

For the evaluation of the effects of the tested OXs on P-gp activity 24 h after pre-exposure, SW480 cells were seeded onto 24-well plates, at a density of 50,000 cells/cm² to

obtain confluent monolayers at the day of the experiment. Three days after seeding, and after reaching confluence, the old cell culture medium was removed, and the cells pre-exposed to **OX 1–6** (20 μM) in fresh cell culture medium for 24 h. After this 24 h incubation period, the cell culture medium containing the compounds was removed, the cells washed with HBSS (+/+), and then submitted to the following procedures:

- RHO 123 accumulation under normal conditions (NA): the cells were pre-incubated with HBSS (+/+), for 30 min at 37 °C, and then further incubated with RHO 123 (5 μM) for 90 min, at 37 °C, in a humidified 5% CO_2 –95% O_2 air atmosphere.
- RHO 123 accumulation in the presence of the P-gp inhibitor (IA): the cells were exposed to the specific P-gp inhibitor, ZOS (10 μM), prepared in HBSS (+/+), for 30 min at 37 °C, and then further incubated with RHO 123 (5 μM) for 90 min, at 37 °C, in a humidified 5% CO_2 –95% O_2 air atmosphere.

After the 90 min RHO 123 accumulation period, the cells were washed twice with HBSS (–/–) and lysed with 1% Triton™ X100, for 30 min, in the dark, at room temperature. After the lysis period, the RHO 123 intracellular fluorescence was measured at excitation/emission wavelengths of 485/528 nm, in a multi-well plate reader (PowerWave-X, BioTek Instruments, Vermont, USA) and expressed as FI. The ratio between the FI after IA and the FI of NA was the parameter used for comparison, and the results were expressed as percentage of control cells (Eq. (1)). Six independent experiments were performed, in triplicate.

RHO 123 accumulation assay in the presence of xanthenes (Protocol B)

For the in vitro evaluation of P-gp activity through protocol B, SW480 cells were seeded in 24-well plates at a density of 50,000 cells/cm² to obtain confluent monolayers on the day of the experiment. After reaching confluence (3 days after seeding), the old cell culture medium was removed, and cells were submitted to the following procedures:

- RHO 123 accumulation under normal conditions (NA): the cells were preexposed to a noncytotoxic concentration of OXs (20 μM), prepared in HBSS (+/+), for 30 min at 37 °C, and then further incubated with RHO 123 (5 μM) for 90 min, at 37 °C, in a humidified 5% CO_2 –95% O_2 air atmosphere. Control cells were only exposed to the P-gp fluorescent substrate.
- RHO 123 accumulation in the presence of the P-gp inhibitor (IA): the cells were simultaneously exposed to

a noncytotoxic concentration of the tested OXs (20 μM) and to the specific P-gp inhibitor, ZOS (10 μM), both prepared in HBSS (+/+), for 30 min at 37 °C, and then further incubated with RHO 123 (5 μM) for 90 min, at 37 °C, in a humidified 5% CO_2 –95% O_2 air atmosphere. Control cells were only exposed to the P-gp inhibitor and to the P-gp fluorescent substrate. It should be noted that each of the previously mentioned exposure conditions (NA and IA, in the presence or absence of the tested compounds) were performed in triplicate (three wells for each condition).

After the incubation period, the cells were washed twice with HBSS (–/–) and lysed with 1 % Triton™ X100 for 30 min, in the dark, and at room temperature. After the cells lysis, the RHO 123 intracellular fluorescence was measured at excitation/emission wavelengths of 485/528 nm, in a multi-well plate reader (PowerWave-X, BioTek Instruments, Vermont, USA) and expressed as FI. The ratio between the FI after inhibited RHO 123 accumulation (IA) and the FI of non-inhibited RHO 123 accumulation (NA) was the parameter used for comparison, and the results were expressed as percentage of control cells (Eq. (1)). Five independent experiments were performed, in triplicate.

Evaluation of xanthenes protective effects against MTX-induced cytotoxicity

To evaluate the potential protective effects of OXs against the cytotoxicity elicited by P-gp substrates, MTX was used as a model of a highly toxic P-gp substrate (Consoli et al. 1997; Shen et al. 2009). For that purpose, SW480 cells were seeded in 96-well plates at a density of 50,000 cells/cm² and exposed, after reaching confluence, to MTX (0; 0.1; 0.5; 1; 2.5; 5.0; 10; 25; 50; 100, and 150 μM) in the presence or absence of the studied OXs (20 μM). Twenty-four hours after exposure, the MTX cytotoxicity was evaluated by the NR uptake assay as described in section “Neutral Red uptake assay”. Four independent experiments were performed, in triplicate. However, for this procedure, the xanthonic derivatives were divided into two groups of experiments: group 1, comprising **OX1**, **OX2**, and **OX6**, and group 2, comprising **OX3**, **OX4**, and **OX5**. Both groups showed similar MTX cytotoxicity curves (Fig. S4), making comparisons possible.

The potential protective effect mediated by the test compounds against MTX cytotoxicity was also evaluated in the Caco-2 cell line. For this purpose, MTX (500, 1000, and 1500 μM) cytotoxicity was assessed, also by the NR uptake assay, with or without simultaneous exposure to the tested xanthenes (20 μM), for 24 h. The assay was performed as mentioned for the SW480 cells, although with higher MTX concentrations being tested, given the higher resistance of

Caco-2 cells to MTX-induced cytotoxicity (Peters and Roelofs 1992). Two independent experiments were performed, in triplicate.

A second experimental design of incubation with MTX was also performed for some of the tested OXs. For that purpose, SW480 cells were seeded in 96-well plates at a density of 50,000 cells/cm² and exposed, after reaching confluence, to MTX (0; 5; 10; 50; 100, and 250 μM) for 4 h. After this incubation, the P-gp substrate was removed, the cells washed with HBSS (+/+), followed by the exposure to **OX1** and **OX6** (20 μM) for 20 h. Twenty-four hours after exposure to MTX (4 h MTX + 20 h OXs), the cytotoxicity of the P-gp substrate was evaluated by the NR uptake assay as described in section “Neutral Red uptake assay”. In these experiments, ZOS (5 μM) was used as a model of a P-gp inhibitor, and its effects on MTX cytotoxicity evaluated in the presence or absence of the tested **OX1** and **OX6**. Four independent experiments were performed, in triplicate.

Statistical analysis

GraphPad Prism 6 for Windows (GraphPad Software, San Diego, CA, USA) was used to perform all statistical calculations. Three tests were performed to evaluate the normality of the data distribution: KS, D’Agostino & Pearson omnibus and Shapiro–Wilk normality tests. For data with parametric distribution, One-way ANOVA was used to perform the statistical comparisons, followed by the Dunnett’s multiple comparisons test. For data with only two groups (e.g., RHO 123 cytotoxicity), the statistical comparisons were made using the Unpaired *t* test. Statistical comparisons between groups in experiments with two variables (e.g., MTX cytotoxicity assays) were made using Two-way ANOVA, followed by the Sidak’s multiple comparison *post hoc* test. Details of the performed statistical analysis are described in each figure legend. Differences were considered to be significant for *p* values lower than 0.05.

Docking study

The human P-gp model built using 4Q9H mice P-gp as template has already been published (Martins et al. 2019). The 3D structures of the six test molecules and MTX were drawn using HyperChem 7.5 (Froimowitz 1993), being minimized by the semi-empirical Polak–Ribiere conjugate gradient method (RMS < 0.1 kcal/Å mol) (Kumar et al. 2017, 2019). Docking simulations between the P-gp model and the small molecules were undertaken in AutoDock Vina (Scripps Research Institute, USA) (Trott and Olson 2009, Seeliger and de Groot 2010). AutoDock Vina considered the target conformation as a rigid unit while the ligands were allowed to be flexible and adaptable to the target. Vina searched for the lowest binding affinity

conformations and returned 9 different conformations for each ligand. AutoDock Vina was run using an exhaustiveness of 10 and a grid box with the dimensions of 37.0, 30.0, and 40.0 Å, engulfing the channel formed by the transmembrane domains. Conformations and interactions were visualized using PyMOL version 1.3 (Lill and Danielson 2010).

Results

Oxygenated xanthenes cytotoxicity

Oxygenated xanthenes (**OX 1–6**, 0–50 μM) cytotoxicity toward SW480 cells was evaluated by the MTT reduction and NR uptake assays, 24 h after exposure, to select a noncytotoxic concentration to be used in the subsequent studies. In the MTT reduction assay (Fig. 2), no significant cytotoxicity was detected for any of the tested concentrations (0–50 μM) and up to 24 h of exposure to **OX1**, **OX2**, **OX3**, and **OX4**. For **OX5** and **OX6**, no significant effects were observed for concentrations up to 20 μM, but a significant decrease in mitochondrial function was observed for the 50 μM concentration (the MTT reduction significantly decreased to 87% and 85% for **OX5** and **OX6**, respectively, when compared with control cells).

Concerning the NR uptake assay (Fig. 3), no significant effects on the NR uptake were observed after 24 h of exposure to **OX2**, **OX4**, and **OX6**, for all the tested concentrations (0–50 μM). However, for **OX1**, **OX3**, and **OX5**, a small but significant decrease in the NR uptake was observed for the highest tested concentration (50 μM). Indeed, after 24 h of exposure to 50 μM **OX1**, **OX3**, and **OX5**, the NR uptake significantly reduced to 94%, 93%, and 96%, respectively, when compared with control cells.

According to the obtained results, the concentration of 20 μM was selected for the subsequent experiments given the lack of significant cytotoxicity (Figs. 2, 3). Furthermore, this noncytotoxic concentration was already reported for the studied compounds and for similar xanthonic and thioxanthonic derivatives as a concentration able to cause a significant increase in P-gp expression and/or activity, although in another *in vitro* model, the Caco-2 cells (Silva et al. 2014a; b, 2015a; b; Lopes et al. 2018; Martins et al. 2019).

Oxygenated xanthenes effects on P-gp expression

The ability of the newly synthesized compounds (20 μM) to change P-gp expression in SW480 cells was evaluated by flow cytometry, 24 h after exposure, using a P-gp monoclonal antibody conjugated with PE (UIC2-PE), as previously described (Silva et al. 2014a; b; 2015a; b; Lopes et al. 2018; Martins et al. 2019).

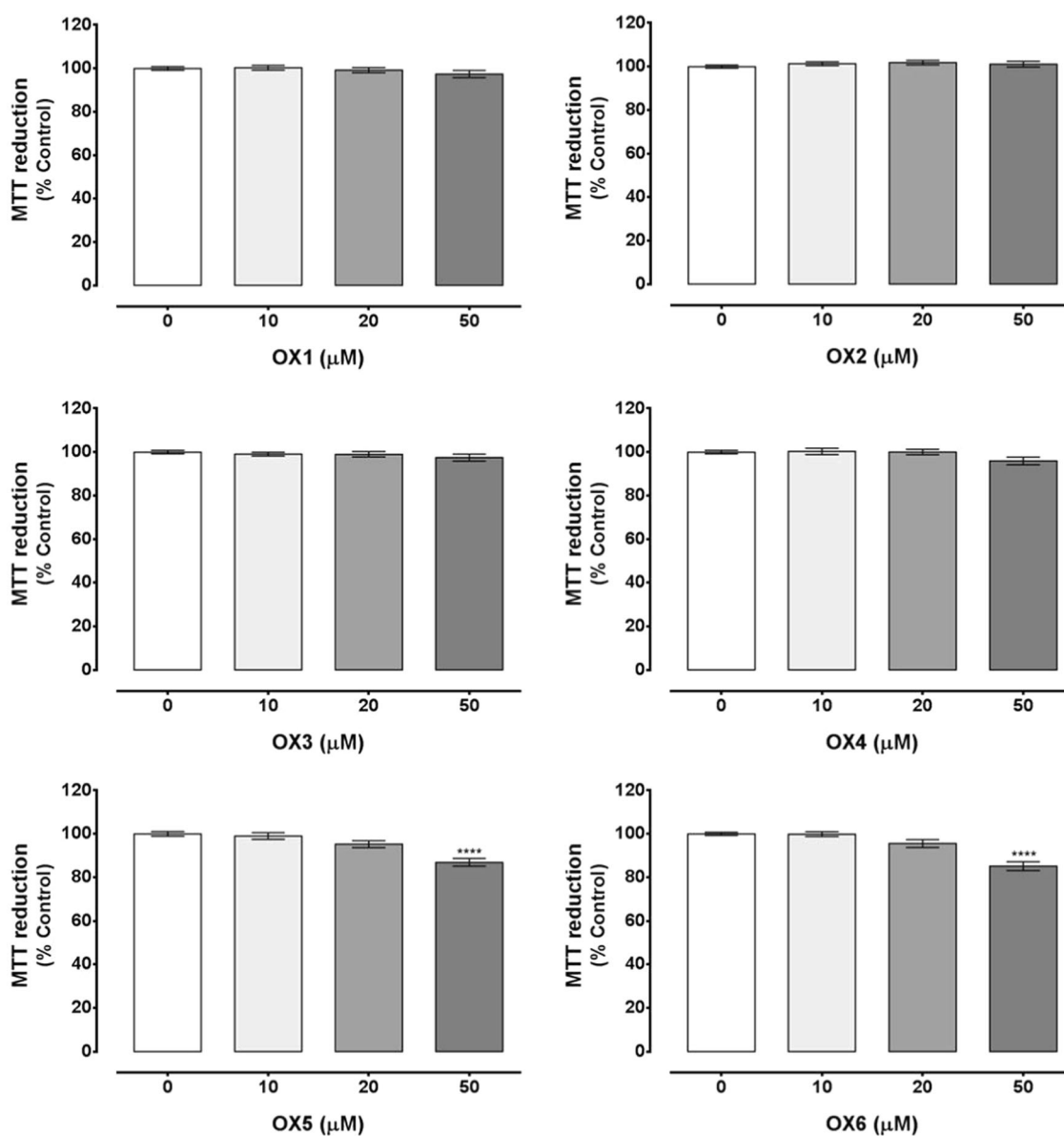


Fig. 2 Oxygenated xanthenes (**OX 1–6**, 0–50 μM) cytotoxicity in SW480 cells evaluated by the MTT reduction assay, 24 h after exposure. Results are presented as mean \pm SEM from six independent experiments, performed in triplicate. Statistical comparisons were

made using the parametric method of One-way ANOVA, followed by the Dunnett's multiple comparisons test [**** $p < 0.0001$ vs. control (0 μM)]

As shown in Fig. 4, **OX2**, **OX4**, **OX5**, and **OX6** significantly increased P-gp expression to 139%, 119%, 113% and 122%, respectively, when compared with control cells (0 μM , 100%). For the remaining xanthonic derivatives, namely **OX1** and **OX3**, no significant effects on P-gp expression were observed after 24 h of exposure. Thus, from the obtained results, **OX2** was the most potent P-gp inducer among the tested compounds (Fig. 4). Representative histograms of flow cytometry analysis of P-gp expression 24 h after exposure of SW480 cells to **OX2** are depicted in Supplementary Fig. S1.

Oxygenated xanthenes effects on P-gp activity

Prior to the evaluation of the tested compounds effects on P-gp activity, the cytotoxicity of the P-gp inhibitor (ZOS: 0–10 μM) and substrate (RHO 123: 0–5 μM) was evaluated in SW480 cells, by the MTT reduction and NR uptake assays. No significant cytotoxicity was observed for ZOS and RHO 123, in both methodologies, for any of the tested concentrations and time-points (24 h and 2 h, respectively), when compared with control cells (Figs. S2, S3). Based on these results, P-gp transport activity

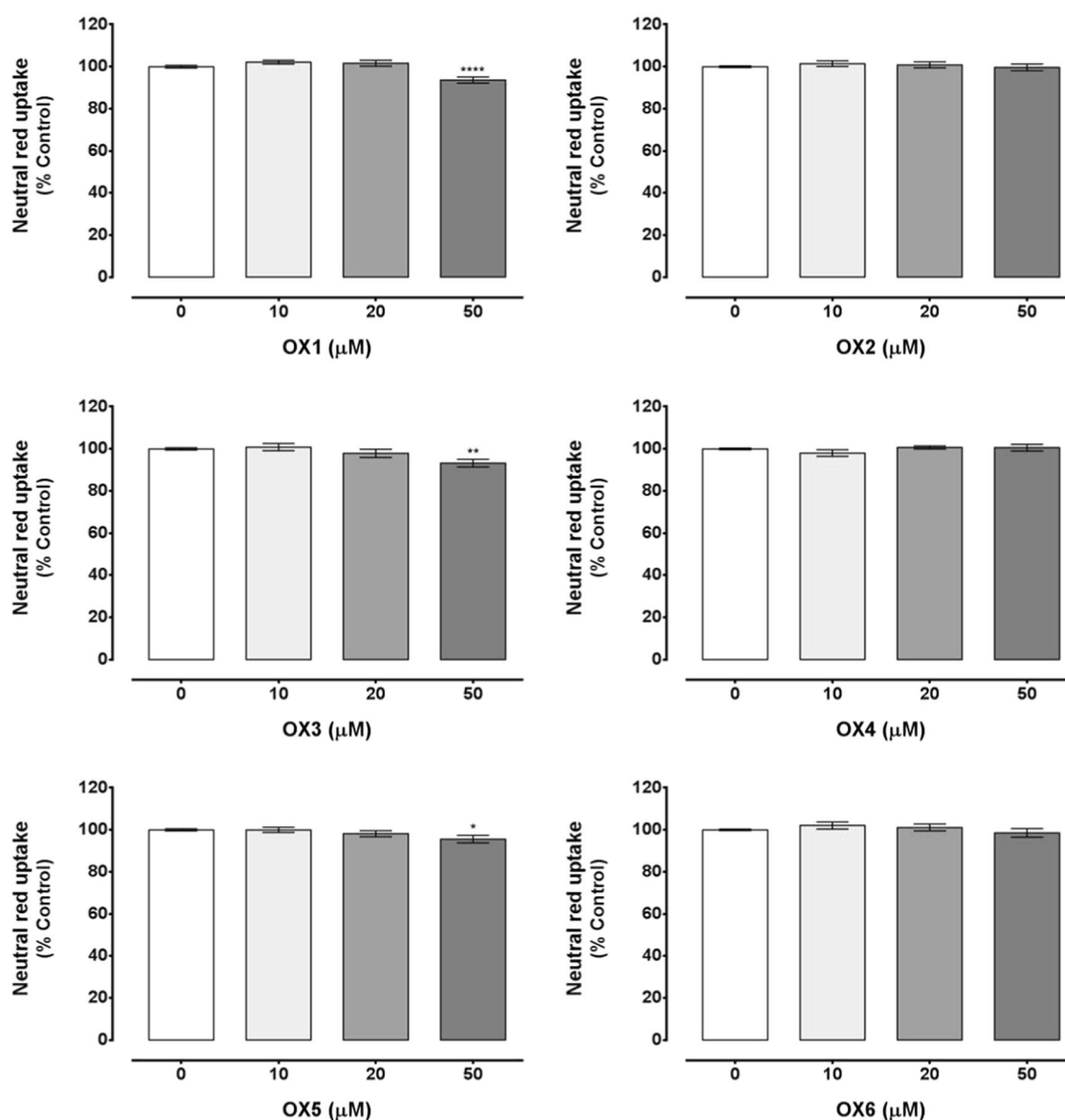


Fig. 3 Oxygenated xanthenes (OX 1–6, 0–50 μM) cytotoxicity in SW480 cells evaluated by the neutral red uptake assay, 24 h after exposure. Results are presented as mean ± SEM from six independent experiments, performed in triplicate. Statistical comparisons were

made using the parametric method of One-way ANOVA, followed by the Dunnett’s multiple comparisons test [$*p < 0.05$; $**p < 0.01$; $****p < 0.0001$ vs. control (0 μM)]

can be safely assessed using 10 μM ZOS and 5 μM RHO 123.

The effect of the newly synthesized compounds on P-gp transport activity was evaluated using two different experimental approaches (Protocol A and B), both using the well-known P-gp fluorescent substrate, RHO 123, and a specific third-generation P-gp inhibitor, ZOS (Vilas-Boas et al. 2011, 2013a; b; Silva et al. 2014a; b; 2015a; b; Lopes et al. 2018).

In the first experimental approach (Protocol A), RHO 123 accumulation was evaluated in SW480 cells preexposed to the test compounds (20 μM) for 24 h. Accordingly, prior to the RHO 123 accumulation phase, the cell culture medium

containing the tested OXs was removed and the cells were washed with HBSS. With this protocol, it is possible to evaluate whether the potentially increased (or decreased) P-gp expression caused by the xanthonic derivatives could be translated into a significantly increased (or decreased) P-gp activity. This fact is of utmost importance since an increased P-gp protein expression does not necessarily translates into an increased transport activity (Takara et al. 2009; Silva et al. 2011, 2014a; b; Vilas-Boas et al. 2011).

As observed in Fig. 5, P-gp activity significantly increased to 133% and 130% in SW480 cells preexposed to OX1 and OX5 for 24 h, respectively. The xanthonic derivatives OX2 and OX6, although to a lower extent, also

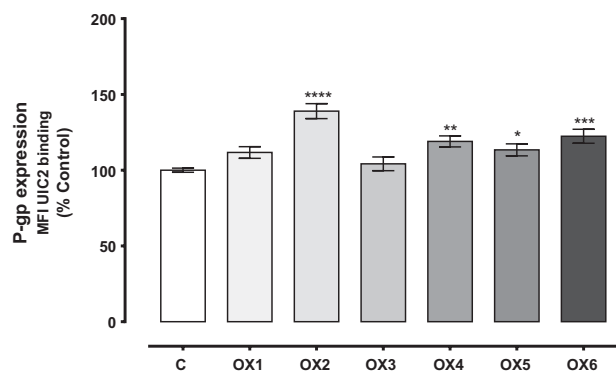


Fig. 4 P-glycoprotein expression evaluated by flow cytometry in SW480 cells, 24 h after exposure to the oxygenated xanthenes **OX 1–6** (20 μ M). Results are presented as mean \pm SEM from six independent experiments, performed in duplicate. Statistical comparisons were made using the parametric method of One-way ANOVA, followed by the Dunnett's multiple comparisons test [$*p < 0.05$; $**p < 0.01$; $***p < 0.001$; $****p < 0.0001$ vs. control (0 μ M)]

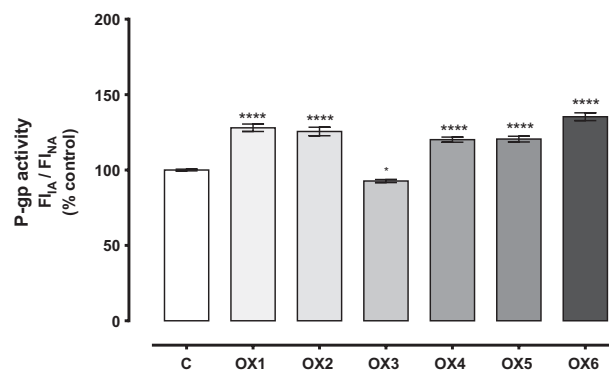


Fig. 6 P-glycoprotein activity evaluated by fluorescence spectroscopy in SW480 cells exposed to the oxygenated xanthenes **OX 1–6** (20 μ M) only during the 90 min incubation period with the fluorescent substrate (5 μ M RHO 123). Results are presented as mean \pm SEM from five independent experiments, performed in triplicate. Statistical comparisons were made using the parametric method of One-way ANOVA, followed by the Dunnett's multiple comparisons test [$*p < 0.05$; $****p < 0.0001$ vs. control (0 μ M)]

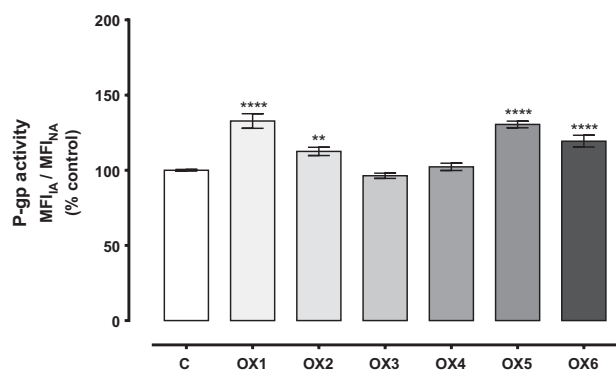


Fig. 5 P-glycoprotein activity evaluated by fluorescence spectroscopy in SW480 cells preexposed to the oxygenated xanthenes **OX 1–6** (20 μ M) for 24 h. Results are presented as mean \pm SEM from six independent experiments, performed in triplicate. Statistical comparisons were made using the parametric method of One-way ANOVA, followed by the Dunnett's multiple comparisons test [$**p < 0.01$; $****p < 0.0001$ vs. control (0 μ M)]

significantly increased P-gp activity to 113% and 119%, respectively. Contrarily, the **OX3** and **OX4** compounds showed no ability to increase the activity of the efflux pump 24 h after exposure (Fig. 5).

In Protocol B, where RHO 123 accumulation in SW480 cells was assessed after 90 min of RHO 123 incubation in the presence of the tested compounds (20 μ M), the results demonstrated that **OX1**, **OX2**, **OX4**, **OX5**, and **OX6** significantly increased P-gp activity (Fig. 6). From the tested compounds, **OX1**, **OX2**, and **OX6** were the most efficient P-gp activators, as revealed by the significantly increased P-gp activity (128%, 126% and 135 %, respectively), when compared with control cells (0 μ M). The derivatives **OX4** and **OX5**, although to a lower extent, also significantly increased P-gp activity to 120% and 121%, respectively, thus also

indicating a potential for P-gp activation. On the other hand, the derivative **OX3** caused a small but significant decrease in P-gp activity. Indeed, **OX3** demonstrated the ability to reduce RHO 123 efflux, increasing the intracellular accumulation of the fluorescent substrate, thus slightly reducing P-gp activity to 93%, when compared with control cells (Fig. 6).

Oxygenated xanthenes effects on MTX cytotoxicity

SW480 cells were further incubated with the toxic P-gp substrate, MTX (0; 0.1; 0.5; 1; 2.5; 5; 10; 25; 50; 100 and 150 μ M), in the presence or absence of the tested OXs (20 μ M), for 24 h. This study aimed to evaluate the potential OXs-mediated protective effect against MTX-induced cytotoxicity, as a result of the previously observed increases in P-gp expression and/or activity.

As shown in Fig. 7, after simultaneous incubation of SW480 cells with MTX (0–150 μ M) and **OX3**, a significant increase in NR uptake was observed for the 2.5 and 25 μ M MTX concentrations, when compared with cells incubated with MTX alone, demonstrating a small but significant protection of SW480 cells against MTX cytotoxic effects. For **OX2**, a small but significant protection against MTX-induced cytotoxicity was observed only for the 5 μ M MTX concentration, when compared with the cells incubated only with the P-gp substrate. On the contrary, **OX5**, when simultaneously incubated with MTX, significantly increased the cytotoxicity of the substrate at the 50 and 100 μ M concentrations, in comparison with the cells incubated with MTX alone. For the other tested compounds, namely **OX1**, **OX4**, and **OX6**, their simultaneous incubation with MTX did not produce significant differences in the cytotoxicity of the substrate, when compared with cells

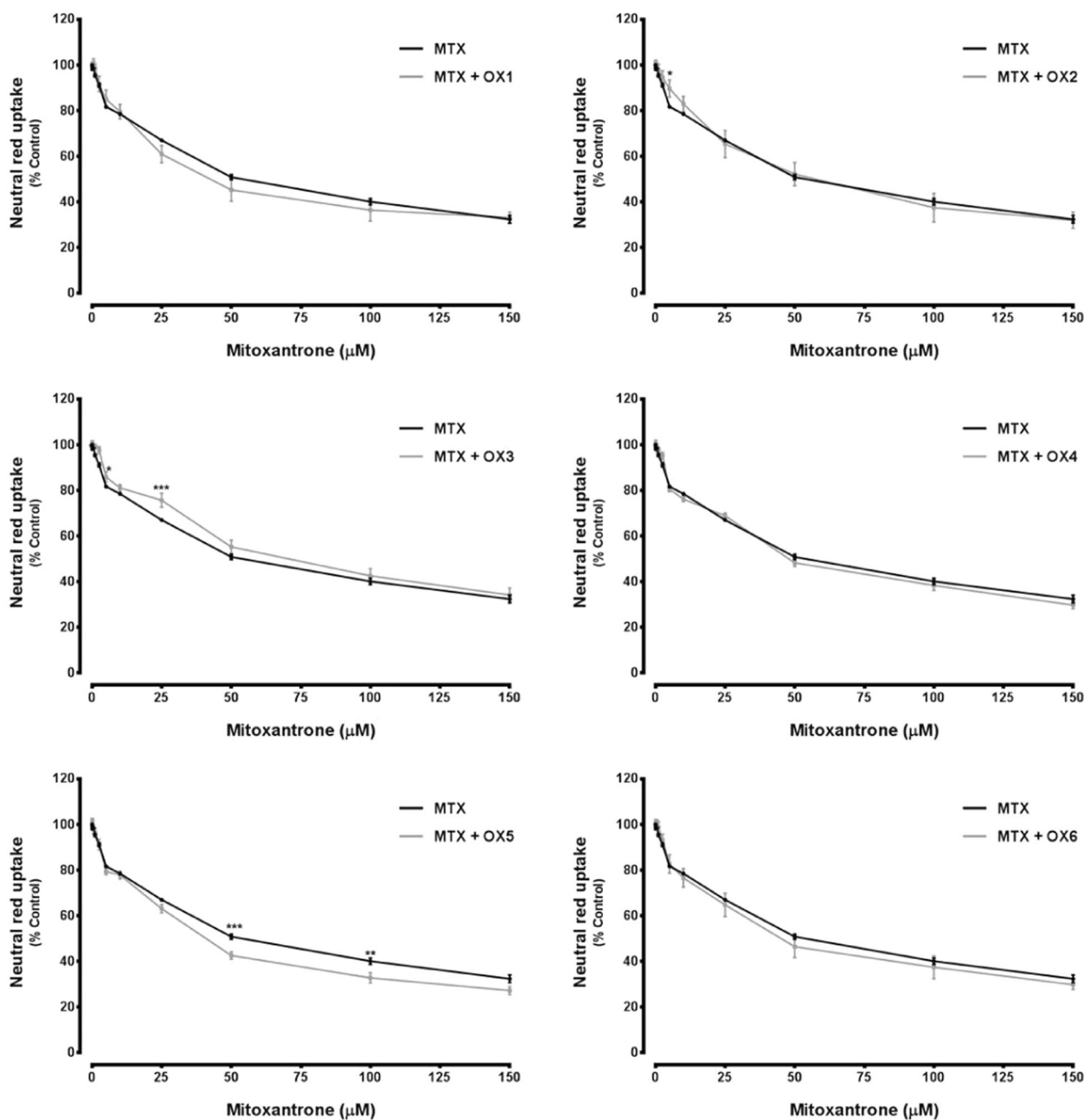


Fig. 7 Mitoxantrone (0–150 µM) cytotoxicity in SW480 cells evaluated by the neutral red uptake assay, with or without simultaneous exposure to the oxygenated xanthenes **OX 1–6** (20 µM) for 24 h. Results are presented as mean ± SEM from four independent

experiments, performed in triplicate. Statistical comparisons were made using Two-way ANOVA, followed by the Sidak’s multiple comparisons test [**p* < 0.05; ***p* < 0.01; ****p* < 0.001 vs. MTX alone]

incubated with MTX alone. From this analysis, it can be concluded that, despite the ability of **OX1**, **OX2**, and **OX6** to significantly increase P-gp activity, being previously considered as the most efficient P-gp activators (Fig. 6), these compounds were not able to markedly protect SW480 cells against the MTX-induced cytotoxicity.

To evaluate whether the lack of protection could be associated with the cell line used [since protection afforded

by **OX2**, **OX3**, **OX4**, and **OX5** was already observed in the Caco-2 cell model, although against another P-gp substrate, the herbicide paraquat (Martins et al. 2019)], the MTX cytotoxicity was also evaluated in Caco-2 cells, in the presence or absence of the tested OXs. The MTX concentrations tested were selected based on EC₅₀ described in the literature, which demonstrated the higher resistance of Caco-2 cells to MTX-induced cytotoxicity (Peters and

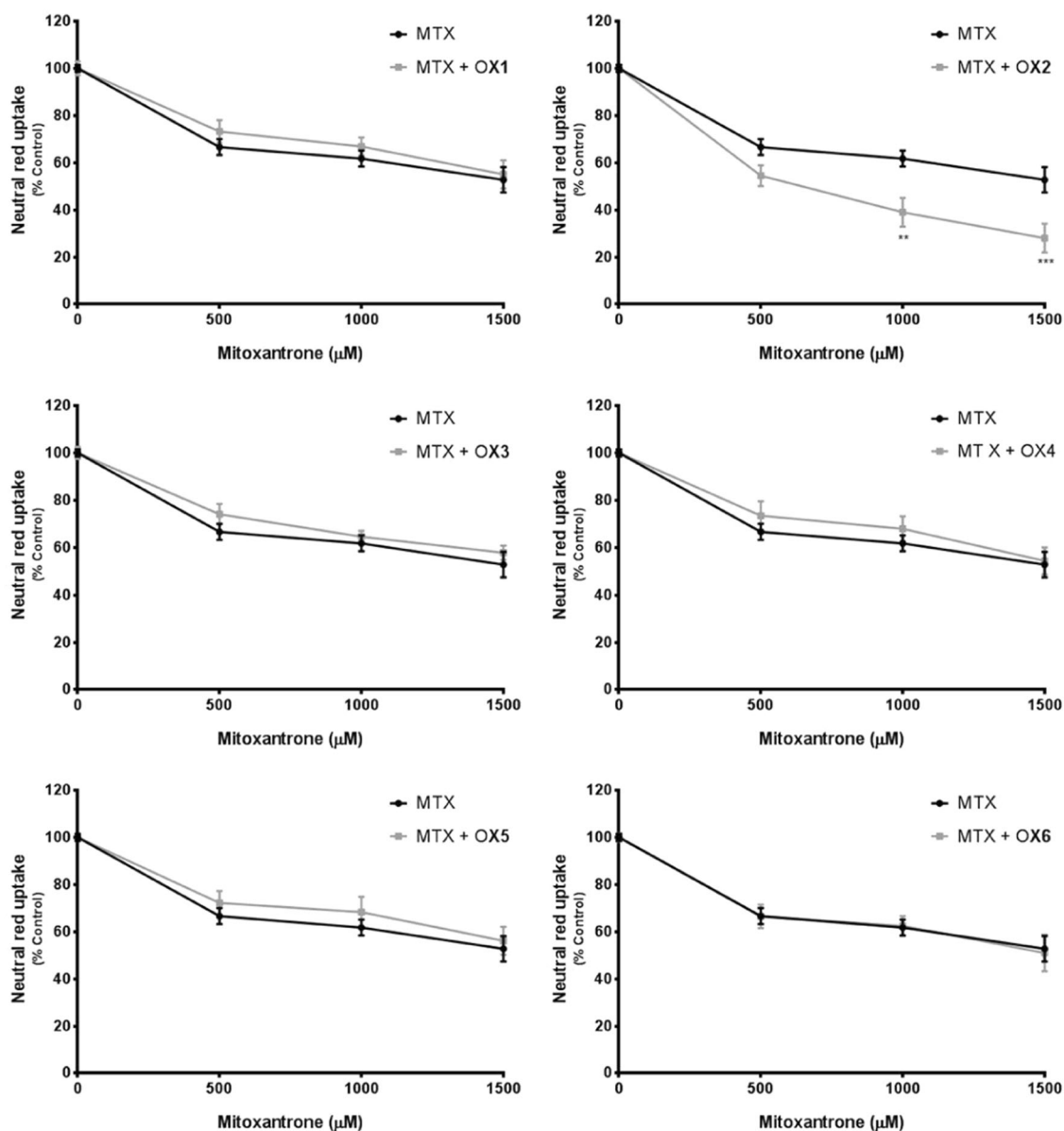


Fig. 8 Mitoxantrone (0–1500 μM) cytotoxicity in Caco-2 cells evaluated by the neutral red uptake assay, with or without simultaneous exposure to the oxygenated xanthenes **OX 1–6** (20 μM) for 24 h. Results are presented as mean \pm SEM from two independent

experiments, performed in triplicate. Statistical comparisons were made using Two-way ANOVA, followed by the Sidak's multiple comparisons test [$**p < 0.01$; $***p < 0.001$ vs. MTX alone]

Roelofs 1992). As shown in Fig. 8, **OX1**, **OX3**, **OX4**, **OX5**, and **OX6** were not able to afford protection against MTX (0–1500 μM) cytotoxicity, when compared with cells incubated with MTX alone. In turn, **OX2**, when simultaneously incubated with MTX (1000 and 1500 μM), caused a significant increase in the substrate cytotoxicity, when comparing to cells incubated with MTX alone.

Given the obtained results, MTX cytotoxicity was tested using a different experimental approach, where SW480 cells were exposed to the P-gp substrate for 4 h, followed by its removal and addition of fresh cell culture medium,

in the presence or absence of **OX1** and **OX6**, the most efficient P-gp activators (Fig. 6), and with or without ZOS-mediated P-gp inhibition. As depicted in Fig. 9, no significant differences were observed in MTX-induced cytotoxicity in the presence or absence of **OX1** and **OX6**, except for the 250 μM MTX concentration where a significant increase in the substrate cytotoxicity was observed upon incubation with **OX6**. Furthermore, the substrate cytotoxicity significantly increased upon ZOS incubation, further demonstrating P-gp involvement in MTX cytotoxicity.

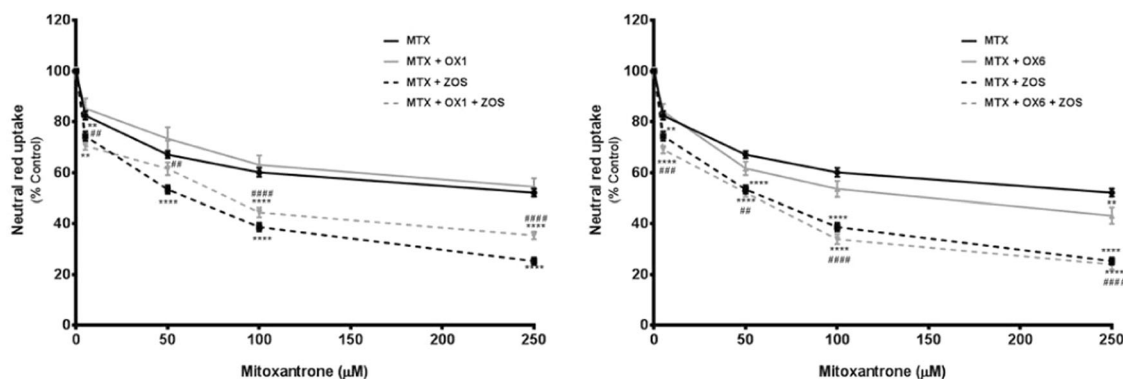


Fig. 9 Mitoxantrone (0–250 μM) cytotoxicity in SW480 cells evaluated by the neutral red uptake assay, after incubation with the substrate for 4 h, followed by its removal and by incubation with and without **OX1** or **OX6** (20 μM) for an additional 20 h, in the presence and absence of ZOS (5 μM). Results are presented as mean \pm SEM

Docking of oxygenated xanthenes and MTX in a human P-gp model

In order to understand the absence/weak OXs-mediated protection against MTX cytotoxicity observed in both SW480 and Caco-2 cells, a docking study on a previously published human P-gp model was performed (Martins et al. 2019). Docking scores obtained range from 6.6 to 7.0 kcal mol⁻¹ (Table 1). A thorough visual inspection revealed that MTX and **OX 1–6** docked on different locations within the drug-binding pocket (Fig. 10a). In fact, from the nine obtained docking poses, the top eight conformations of MTX were located on the TMD (transmembrane domain) interface closer to the nucleotide binding domain (NBD) (binding site I, Fig. 10a), and therefore, closer to the cell surface; **OX 1–6** are predicted to bind preferably on Binding site II (Fig. 10a), located on the TMD interface inside the cellular membrane. According to the *in silico* study, MTX establishes polar interactions with residues Asp167, Glu170, Thr173, Arg174, Asp178, Lys181, and Asn357; **OX 1–6** establish π -stacking interactions with Phe-938, and polar interactions with several residues, such as Asp188, Lys189, Gly187, Glu184, Asn183, Ala883, Leu879, and Lys934 (Fig. 10b).

Discussion

P-gp is an extremely important ABC transporter, not only for the maintenance of cellular homeostasis but also for the detoxification of substances with toxic potential (Silva et al. 2015a; b). For this reason, several compounds, including (thio)xanthonic derivatives, have been extensively studied for their ability to increase P-gp expression and/or activity and, consequently, to afford protection against its toxic substrates (Silva et al. 2014a; b; 2015a; b;

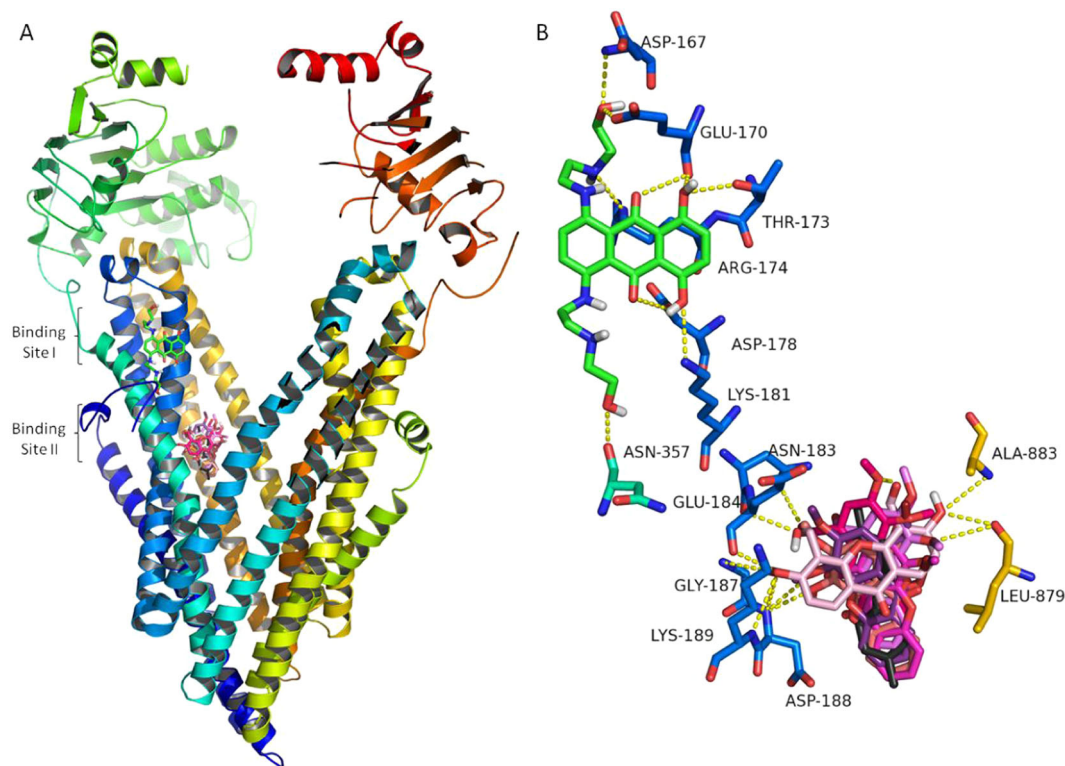
from four independent experiments, performed in triplicate. Statistical comparisons were made using Two-way ANOVA, followed by the Sidak's multiple comparisons test [$**p < 0.01$; $****p < 0.0001$ vs. MTX alone; $\#p < 0.01$; $\###p < 0.001$; $\####p < 0.0001$ MTX + OXs vs. MTX + OXs + ZOS]

Lopes et al. 2018, Martins et al. 2019, Rocha-Pereira et al. 2019). Therefore, the main goal of this study was to investigate, using the human colorectal SW480 cells, the potential of six OX to increase P-gp expression and/or activity at the intestinal barrier, which could be further explored and proposed as antidotes in intoxications caused by toxic P-gp substrates.

The results demonstrated that the studied **OX 1–6** did not show significant cytotoxicity toward SW480 cells, after 24 h of exposure, and for concentrations up to 20 μM (Figs. 2, 3). In accordance with these results, this noncytotoxic concentration was selected to further evaluate the effects of OXs on P-gp expression and activity. Furthermore, and as previously mentioned, this concentration was already reported in the literature for similar (thio)xanthonic derivatives as a concentration that causes a positive P-gp modulatory effect (Silva et al. 2014a; b; 2015a; b; Lopes et al. 2018; Martins et al. 2019; Rocha-Pereira et al. 2019). In the present study, some of the tested compounds (**OX1**, **OX2**, **OX4**, **OX5**, and **OX6**) showed the capacity to immediately increase P-gp activity in SW480 cells, thus behaving as P-gp activators (Fig. 6). On the opposite, **OX3** was shown to slightly but significantly decrease the activity of the efflux pump, after a short incubation with RHO 123. In accordance with the obtained data, similar results were previously reported in Caco-2 cells, with all the tested xanthenes, except **OX3**, significantly and immediately increasing P-gp activity, when compared with control cells (Martins et al. 2019). Furthermore, although previous studies already reported the potential of xanthonic derivatives, including **OX 1–6**, for P-gp activation in Caco-2 cells (Silva et al. 2014a; b; Martins et al. 2019), to the best of our knowledge this is the first report on the ability of xanthonic derivatives to immediately increase P-gp activity in SW480 cells, further validating the use of this *in vitro* model for the screening of P-gp activators.

Table 1 Docking scores for the six tested oxygenated xanthenes (**OX 1–6**) and mitoxantrone on P-gp transmembrane domains (TMDs)

Ligand	Free energy of ligand: P-gp TMD complex (kcal mol ⁻¹)	Nr of docked results on Binding site I (Total of 9)	Nr of docked results on Binding site II (Total of 9)	Nr of docked results on other locations (Total of 9)
OX1	-6.6	0	9	0
OX2	-7.0	0	9	0
OX3	-6.7	1	8	0
OX4	-6.7	1	7	1
OX5	-6.7	0	9	0
OX6	-6.7	0	9	0
Mitoxantrone	-6.9	8	1	0

**Fig. 10** **a** Ribbon representation of human P-gp model; mitoxantrone (Binding site I) and **OX 1–6** (Binding site II) are docked to the transmembrane domains. **b** Detailed view of mitoxantrone (greensticks) and **OX 1–6** (pink sticks) on Binding sites I and II, respectively. Polar interactions are depicted as yellow broken lines and residues evolved are labeled

In addition, **OX2**, **OX4**, **OX5**, and **OX6** significantly increased cell-surface P-gp expression in SW480 cells 24 h after exposure [since the monoclonal antibody recognizes an external P-gp epitope (Vilas-Boas et al. 2011, Silva et al. 2014a; b)], thus demonstrating to be P-gp inducers (Fig. 4). For **OX2**, **OX5**, and **OX6**, the observed increases in cell-surface P-gp expression were accompanied by significant increases in P-gp transport activity after 24 h of pre-exposure, although to a lower extent in cells preexposed to **OX2** (Fig. 5). Furthermore, **OX1** significantly increased P-gp activity in SW480 cells preexposed to the xanthonic derivative for 24 h, although no significant effects were

observed in cell-surface P-gp expression. Since **OX1** was confirmed as a P-gp activator (Fig. 6), the significant increase in P-gp activity, observed in cells preexposed to **OX1** for 24 h, may result from a direct pump activation mediated by the compound that remained intracellularly, instead of resulting from an increased P-gp expression. Furthermore, for **OX4**, the observed increase in the cell-surface P-gp expression did not result into a significant increase in protein transport activity 24 h after exposure. Thus, although the *de novo* synthesized P-gp is already incorporated into the plasma membrane, it may not yet be fully functional. Taken together, these results reinforce the

importance of the simultaneous determination of both P-gp expression and activity in the screening of P-gp inducers, since an increased protein expression does not necessarily translate into an increased transport activity, and increases in efflux activity can be observed independently of the level of expression, as already demonstrated in previous *in vitro* and *in vivo* studies (Silva et al. 2011, 2014a; b; Vilas-Boas et al. 2011; Rocha-Pereira et al. 2019). Noteworthy, to the best of our knowledge, this is the first report on the ability of xanthonic derivatives to significantly increase P-gp expression in SW480 cells, validating SW480 cells as a suitable *in vitro* model for the screening and selection of P-gp inducers. Moreover, when comparing the obtained results with the previous studies performed in Caco-2 cells, a higher responsiveness to possible P-gp inducers was observed in the SW480 cells, with four out of six OXs demonstrating a potential for P-gp induction (**OX2**, **OX4**, **OX5**, and **OX6**).

The present study also aimed to evaluate the potential protective effect of each OX against the cytotoxicity caused by MTX, a P-gp highly toxic substrate. However, none of the tested compounds that positively modulated P-gp expression and/or activity markedly protected SW480 cells against the cytotoxicity induced by MTX. Moreover, and unexpectedly, **OX5** exacerbated MTX cytotoxicity in SW480 cells, 24 h after simultaneous incubation with the P-gp substrate. Furthermore, the simultaneous incubation of MTX and **OX3** resulted in a reduction in the MTX-mediated cytotoxicity. Given the lack of positive modulatory effects of **OX3** on P-gp activity, mechanisms other than P-gp modulation may be responsible for the observed protection.

Since some of the tested OXs, namely **OX2**, **OX4**, and **OX5**, by significantly increasing P-gp expression and activity in Caco-2 cells, caused a significant protection against PQ-induced cytotoxicity (Martins et al. 2019), it was hypothesized that the lack of relevant protection against MTX cytotoxicity observed in the present study could be related with the *in vitro* model used. Therefore, MTX cytotoxicity was also evaluated in Caco-2 cells, although at higher MTX concentrations given their higher resistance to the substrate-induced cytotoxicity (Peters and Roelofs 1992). However, and as demonstrated for SW480 cells, the tested OXs were not able to significantly protect Caco-2 cells against MTX-induced cytotoxicity and **OX2** was even able to significantly increase its cytotoxic effect.

P-gp is a single polypeptide composed by two homologous halves, each one comprising one transmembrane domain [TMD, composed of six transmembrane α -helices] and one NBD, which couples the energy associated with ATP binding and hydrolysis to drug transport (Rosenberg et al. 2005). Using a validated human P-gp model, we thus sought to understand the absence/weak OXs-mediated protection against MTX cytotoxicity. According to the obtained

data, the absence or very mild influence of the tested OXs on MTX-induced cytotoxicity may be related to the different binding locations. In fact, a P-gp large common binding site had been initially proposed (Borgnia et al. 1996), but later several binding sites were suggested to explain the behavior of P-gp when co-transport of several substrates takes place, or when cooperative, competitive, and noncompetitive interactions with MDR modulators were observed (Martin et al. 2000; Safa 2004). Although MTX has been described as a P-gp substrate (Consoli et al. 1997), in certain P-gp-positive cell lines, in presence of a P-gp inhibitor, there is no effect on MTX sensitivity (Asschert et al. 1997). However, in this study we demonstrated a significant increase in MTX-mediated cytotoxicity upon P-gp inhibition with ZOS, a potent third-generation P-gp inhibitor.

The weak OXs-mediated protection against MTX toxicity may also be due to other mechanisms evolved, as MTX is also a substrate of other transporters, such as BRCP and MRP-1 (Mitra and Audus 2010).

In conclusion, it was clearly demonstrated the ability of OXs for P-gp positive modulation (expression and activity) at the intestinal level, opening new perspectives to mechanistically explore the physiological role of this transporter. Furthermore, the SW480 cells demonstrated to be an appropriate *in vitro* model to be used in the screening of P-gp inducers and activators. Knowing that P-gp induction and/or activation may represent a potential antidotal pathway in cases of intoxication by its toxic substrates, and given the *in vitro* potential of these xanthonic derivatives as P-gp activators, this important class of compounds deserves particular attention at the toxicological level, as they can constitute a promising source of novel derivatives that worth to be studied. Furthermore, it is important to additionally investigate the P-gp-mediated transport of its substrates in order to better understand the mechanisms underlying P-gp activation.

Acknowledgements The work was supported by UID/MULTI/04378/2019, UIDB/04423/2020 and UIDP/04423/2020 with funding from FCT/MCTES through national funds and under the projects NORTE-01-0145-FEDER-000024, supported by Norte Portugal Regional Operational Programme (NORTE2020), under the PORTUGAL 2020 Partnership Agreement (DESIGNBIOtecHealth-New Technologies for three Health Challenges of Modern Societies: Diabetes, Drug Abuse and Kidney Diseases) and PTDC/SAU-PUB/28736/2017 (reference POCI-01-0145-FEDER-028736), co-financed by COMPETE 2020, Portugal 2020 and the European Union through the ERDF and by FCT through national funds.

Compliance with ethical standards

Conflict of interest The authors declare that they have no conflict of interest.

Publisher's note Springer Nature remains neutral with regard to jurisdictional claims in published maps and institutional affiliations.

References

- Arbo MD, Silva R, Barbosa DJ, da Silva DD, Rossato LG, Bastos MdL, Carmo H (2014) Piperazine designer drugs induce toxicity in cardiomyoblast h9c2 cells through mitochondrial impairment. *Toxicol Lett* 229(1):178–189
- Asschert J, de Vries E, van der Kolk D, Muller M, Vellenga E (1997) The combined effects of IL-3 and PSC 833 on daunorubicin- and mitoxantrone cytotoxicity in two growth factor-dependent leukemic cell lines. *Leukemia* 11(5):680–686
- Barbosa DJ, Capela JP, Silva R, Ferreira LM, Branco PS, Fernandes E, Bastos ML, Carvalho F (2014) “Ecstasy”-induced toxicity in SH-SY5Y differentiated cells: role of hyperthermia and metabolites. *Arch Toxicol* 88(2):515–531
- Borenfreund E, Babich H, Martin-Alguacil N (1988) Comparisons of two in vitro cytotoxicity assays—the neutral red (NR) and tetrazolium MTT tests. *Toxicol Vitro* 2(1):1–6
- Borgnia MJ, Eytan GD, Assaraf YG (1996) Competition of hydrophobic peptides, cytotoxic drugs, and chemosensitizers on a common P-glycoprotein pharmacophore as revealed by its ATPase activity. *J Biol Chem* 271(6):3163–3171
- Consoli U, Van NT, Neamati N, Mahadevia R, Beran M, Zhao S, Andreeff M (1997) Cellular pharmacology of mitoxantrone in p-glycoprotein-positive and -negative human myeloid leukemic cell lines. *Leukemia* 11(12):2066–2074
- Cruz I, Puthongking P, Cravo S, Palmeira A, Cidade H, Pinto M and Sousa E (2017) Xanthone and flavone derivatives as dual agents with acetylcholinesterase inhibition and antioxidant activity as potential anti-Alzheimer agents. *J Chem* 2017:16 pages
- Fernandes EG, Silva AM, Cavaleiro JA, Silva FM, Fernanda M, Borges M, Pinto MM (1998) ¹H and ¹³C NMR Spectroscopy of mono-, di-, tri- and tetrasubstituted xanthenes. *Magn Reson Chem* 36(4):305–309
- Froimowitz M (1993) HyperChem: a software package for computational chemistry and molecular modeling. *Biotechniques* 14(6):1010–1013
- Fromm MF (2004) Importance of P-glycoprotein at blood-tissue barriers. *Trends Pharm Sci* 25(8):423–429
- Gameiro M, Silva R, Rocha-Pereira C, Carmo H, Carvalho F, Bastos ML, Remião F (2017) Cellular models and in vitro assays for the screening of modulators of P-gp, MRP1 and BCRP. *Molecules* 22:E600
- Gomes S, Raimundo L, Soares J, Loureiro JB, Leao M, Ramos H, Monteiro MN, Lemos A, Moreira J, Pinto M, Chlapek P, Veselska R, Sousa E, Saraiva L (2019) New inhibitor of the TAp73 interaction with MDM2 and mutant p53 with promising antitumor activity against neuroblastoma. *Cancer Lett* 446:90–102
- Kumar N, Goel N, Chand Yadav T, Pruthi V (2017) Quantum chemical, ADMET and molecular docking studies of ferulic acid amide derivatives with a novel anticancer drug target. *Med Chem Res* 26(8):1822–1834
- Kumar N, Gupta S, Chand Yadav T, Pruthi V, Kumar Varadwaj P, Goel N (2019) Extrapolation of phenolic compounds as multi-target agents against cancer and inflammation. *J Biomol Struct Dyn* 37(9):2355–2369
- Lemos A, Gomes AS, Loureiro JB, Brandão P, Palmeira A, Pinto MMM, Saraiva L, Sousa ME (2019) Synthesis, biological evaluation, and in silico studies of novel aminated xanthenes as potential p53-activating agents. *Molecules* 24(10):1975
- Lill MA, Danielson ML (2010) Computer-aided drug design platform using PyMOL. *J Comput Aided Mol Des* 25(1):13–19
- Lopes A, Martins E, Silva R, Pinto MMM, Remião F, Sousa E, Fernandes C (2018) Chiral thioxanthenes as modulators of p-glycoprotein: synthesis and enantioselectivity studies. *Molecules* 23:E626
- Martin C, Berridge G, Higgins CF, Mistry P, Charlton P, Callaghan R (2000) Communication between multiple drug binding sites on P-glycoprotein. *Mol Pharm* 58(3):624–632
- Martins E, Silva V, Lemos A, Palmeira A, Puthongking P, Sousa E, Rocha-Pereira C, Ghanem CI, Carmo H, Remião F, Silva R (2019) Newly synthesized oxygenated xanthenes as potential p-glycoprotein activators: in vitro, ex vivo, and in silico studies. *Molecules* 24(4):707
- Masters KS, Brase S (2012) Xanthenes from fungi, lichens, and bacteria: the natural products and their synthesis. *Chem Rev* 112(7):3717–3776
- Mitra P, Audus KL (2010) MRP isoforms and BCRP mediate sulfate conjugate efflux out of BeWo cells. *Int J Pharm* 384(1–2):15–23
- Mizutani T, Nakamura T, Morikawa R, Fukuda M, Mochizuki W, Yamauchi Y, Nozaki K, Yui S, Nemoto Y, Nagaishi T, Okamoto R, Tsuchiya K, Watanabe M (2012) Real-time analysis of P-glycoprotein-mediated drug transport across primary intestinal epithelium three-dimensionally cultured in vitro. *Biochem Biophys Res Commun* 419(2):238–243
- Oostendorp RL, Beijnen JH, Schellens JH (2009) The biological and clinical role of drug transporters at the intestinal barrier. *Cancer Treat Rev* 35(2):137–147
- Pang KS (2003) Modeling of intestinal drug absorption: roles of transporters and metabolic enzymes (for the Gillette Review Series). *Drug Metab Dispos* 31(12):1507–1519
- Peters WHM, Roelofs HMJ (1992) Biochemical characterization of resistance to mitoxantrone and adriamycin in Caco-2 human colon adenocarcinoma cells: a possible role for glutathione S-transferases. *Cancer Res* 52(7):1886
- Pinto MM, Sousa ME, Nascimento MS (2005) Xanthone derivatives: new insights in biological activities. *Curr Med Chem* 12(21):2517–2538
- Repetto G, del Peso A, Zurita JL (2008) Neutral red uptake assay for the estimation of cell viability/cytotoxicity. *Nat Protoc* 3(7):1125–1131
- Resende D, Pereira-Terra P, Inacio AS, Costa PMD, Pinto E, Sousa E, Pinto MMM (2018) Lichen xanthenes as models for new antifungal agents. *Molecules* 23:E2617
- Rocha-Pereira C, Ghanem CI, Silva R, Casanova AG, Duarte-Araújo M, Gonçalves-Monteiro S, Sousa E, de Lourdes Bastos M, Remião F (2019) P-glycoprotein activation by 1-(propan-2-ylamino)-4-propoxy-9H-thioxanthen-9-one (TX5) in rat distal ileum: ex vivo and in vivo studies. *Toxicol Appl Pharmacol* 386:114832
- Rosenberg MF, Callaghan R, Modok S, Higgins CF, Ford RC (2005) Three-dimensional structure of P-glycoprotein: the transmembrane regions adopt an asymmetric configuration in the nucleotide-bound state. *J Biol Chem* 280(4):2857–2862
- Safa AR (2004) Identification and characterization of the binding sites of P-glycoprotein for multidrug resistance-related drugs and modulators. *Curr Med Chem Anticancer Agents* 4(1):1–17
- Seeliger D, de Groot BL (2010) Ligand docking and binding site analysis with PyMOL and Autodock/Vina. *J Comput Aided Mol Des* 24(5):417–422
- Sharom FJ (2011) The P-glycoprotein multidrug transporter. *Essays Biochem* 50(1):161–178
- Shen F, Bailey BJ, Chu S, Bence AK, Xue X, Erickson P, Safa AR, Beck WT, Erickson LC (2009) Dynamic assessment of mitoxantrone resistance and modulation of multidrug resistance by valspodar (PSC833) in multidrug resistance human cancer cells. *J Pharm Exp Ther* 330(2):423–429
- Silva R, Carmo H, Dinis-Oliveira R, Cordeiro-da-Silva A, Lima SC, Carvalho F, Bastos Mde L, Remião F (2011) In vitro study of P-glycoprotein induction as an antidotal pathway to prevent cytotoxicity in Caco-2 cells. *Arch Toxicol* 85(4):315–326
- Silva R, Carmo H, Vilas-Boas V, Barbosa DJ, Palmeira A, Sousa E, Carvalho F, Bastos Mde L, Remião F (2014a) Colchicine effect

- on P-glycoprotein expression and activity: in silico and in vitro studies. *Chem Biol Interact* 218:50–62
- Silva R, Palmeira A, Carmo H, Barbosa DJ, Gameiro M, Gomes A, Paiva AM, Sousa E, Pinto M, Bastos Mde L, Remiao F (2015a) P-glycoprotein induction in Caco-2 cells by newly synthesized thioxanthenes prevents paraquat cytotoxicity. *Arch Toxicol* 89(10):1783–1800
- Silva R, Sousa E, Carmo H, Palmeira A, Barbosa DJ, Gameiro M, Pinto M, Bastos Mde L, Remiao F (2014b) Induction and activation of P-glycoprotein by dihydroxylated xanthenes protect against the cytotoxicity of the P-glycoprotein substrate paraquat. *Arch Toxicol* 88(4):937–951
- Silva R, Vilas-Boas V, Carmo H, Dinis-Oliveira RJ, Carvalho F, de Lourdes Bastos M, Remiao F (2015b) Modulation of P-glycoprotein efflux pump: induction and activation as a therapeutic strategy. *Pharm Ther* 149:1–123
- Takara K, Hayashi R, Kokufu M, Yamamoto K, Kitada N, Ohnishi N, Yokoyama T (2009) Effects of nonsteroidal anti-inflammatory drugs on the expression and function of P-glycoprotein/MDR1 in Caco-2 cells. *Drug Chem Toxicol* 32(4):332–337
- Trott O, Olson AJ (2009) AutoDock Vina: improving the speed and accuracy of docking with a new scoring function, efficient optimization, and multithreading. *J Comput Chem* 31(2):455–461
- Varma MV, Ambler CM, Ullah M, Rotter CJ, Sun H, Litchfield J, Fenner KS, El-Kattan AF (2010) Targeting intestinal transporters for optimizing oral drug absorption. *Curr Drug Metab* 11(9):730–742
- Vilas-Boas V, Silva R, Gaio AR, Martins AM, Lima SC, Cordeiro-da-Silva A, de Lourdes Bastos M, Remiao F (2011) P-glycoprotein activity in human Caucasian male lymphocytes does not follow its increased expression during aging. *Cytometry Part A* 79(11):912–919
- Vilas-Boas V, Silva R, Nunes C, Reis S, Ferreira L, Vieira C, Carvalho F, Bastos MdL, Remião F (2013a) Mechanisms of P-gp inhibition and effects on membrane fluidity of a new rifampicin derivative, 1,8-dibenzoyl-rifampicin. *Toxicol Lett* 220(3):259–266
- Vilas-Boas V, Silva R, Palmeira A, Sousa E, Ferreira LM, Branco PS, Carvalho F, Bastos Mde L, Remiao F (2013b) Development of novel rifampicin-derived P-glycoprotein activators/inducers. synthesis, in silico analysis and application in the RBE4 cell model, using paraquat as substrate. *PLoS ONE* 8(8):e74425